出國報告（出國類別：國際會議）

主動式孤島偵測法結合智慧型控制器

服務機關：國防大學理工學院電機電子系
姓名職稱：中校教師談光雄
派赴國家：日本
出國期間：105/05/25-105/05/29
報告日期：105/05/27

摘要

2016 年「第 18 屆電機工程與技術國際研討會」(18th International Conference on Electrical Engineering and Technology, ICEET 2016)係由世界科學，工程與技術學院 (World Academy of Science, Engineering and Technology, WASET)舉辦，並於 105 年 5 月 26 日至 27 日在日本東京成田東武機場酒店(Narita Tobu Hotel Airport)舉行，本人投稿該研討會論文乙篇，論文題目：主動式孤島偵測法結合智慧型控制器，因榮獲刊登及大會議程安排於 5 月 27 日上午 1045-1300 場次進行電子海報發表，故於 5 月 25 日搭機前往與會。當日該場次會議中，計有來至台灣、日本、南韓、科威特、法國及墨西哥等十五篇論文發表，期間發表人均詳細報告其研究成果，報告完後，台下與台上學者討論熱絡，彼此交流受益良多。

目次

頁次

壹、目的：

2016 年「第 18 屆電機工程與技術國際研討會」(18th International Conference on Electrical Engineering and Technology, ICEET 2016)，由主辦單位 WASET 於 105 年 5 月 26 日至 27 日在日本東京成田東武機場酒店(Narita Tobu Hotel Airport)舉行，該研討會主要提供科學家，研究人員和學者彼此交流和分享有關電機工程與技術各方面的研究成果與實務經驗。另外，還提供了跨領域之科技人員和教育工作者以介紹和討論其最新的創新技術，趨勢，實務挑戰和解決方法之主要研究平台。而本次參與發表之專家學者，計有來至台灣、日本、南韓、印尼、阿爾及利亞、巴西、泰國、科威特、法國及墨西哥等各國專家學者，合計發表海報與論文達 270 餘篇。藉由參加本次國際研討會，除了平日鑽研研究與查閱期刊論文所得知識，更能開闊眼界，瞭解國際研究趨勢與脈動，進而增進研究動力與方向。此外，本會議所投稿之論文均經由國際相關領域之學者、專家審查，因此一旦獲得大會收錄刊登，亦將大幅增加本院的能見度及學術地位。

貳、過程：

會議議程

May 27, 2016, HALL B : 10:45 – 13:00

Session Chair: Prof. Joselito Medina, Kazuki Hiro

本人發表之論文名稱：

Active Islanding Detection Method Using Intelligent Controller

作者：

Kuang-Hsiung Tan (談光雄), Chih-Chan Hu, Chien-Wu Lan, Shih-Sung Lin, and Te-Jen Chang (Chung Cheng Institute of Technology, National Defense University, ROC)

本次赴日本東京參加國際研討會，因國人赴日本免簽證及當地交通便利之因素，故僅委託旅行社代訂來回機票，而相關住宿則自行決定住宿 APA 上野站前酒店四晚，因研討會舉辦地點成田東武機場酒店在成田機場附近離市區略有相當距離，惟因上野站有京成上野 Skyline 快速地鐵往返機場僅需 30 餘分，因而決定住宿上野站附近之 APA 上野站前酒店以節省開支。研討會舉行時間為 105 年 5 月 26 日至 27 日，故委由旅行社代訂 5 月 25 日上午 04 時 05 分搭乘中華航空 CI0108 班機赴日本成田機場，抵達成田機場時已逾當地時間 8 時 25 分(與台灣時差 1 小時)，辦好出關手續，即自行搭乘京成上野 Skyline 抵達上野站，再步行約 10 分鐘後抵達下榻飯店，此時已逾 10 時 30 分，由於此時飯店仍無法辦理入住，故在辦理寄放行李後，選擇離飯店附近之餐廳用餐並稍作休息，而晚上則在飯店稍作準備與休息。5 月 26 日當日早上 10:10 到達會場並完成報到手續，當日並擇感興趣之場次聆聽相關論文發表。5 月 27 日發表當日早上 09:00 抵達會議地點，電子海報與論文發表場次同為上午 10 時 45 分場次，會議一開始，由會議主持人 Prof. Kazuki Hiro 主持議程並由發表人逐一開始報告，本會議共發表十五篇論文及電子海報發表，分別由墨西哥 Autonomous University of Hidalgo State、南韓 Incheon National University、Korea University、Kyungpook National University、日本 National Institute of Technology、University of Tokyo、法國 Blaise Pascal University 及台灣台北醫學大學等專家學者輪流發表，發表人均詳細報告其研究成果，報告完後，主持人亦提供時間給在場與會專家、學者提問，由於所研究之領域具相關性，因此台下與台上學者討論相當熱絡。本人發表之電子海報為第 6 順位，發表完後，學者亦提出相關見解及寶貴建議，對於本次參加國際研討會，使自身能更瞭解國際研究趨勢與脈動，因此對於未來研究方向將有更多動力。

本人所發表之論文為「Active Islanding Detection Method Using Intelligent Controller」，內容報告摘要如下：本論文提出一種新型主動式孤島偵測法，其係運用注入擾動訊號並結合智慧型控制器以達到孤島偵測目的。首先，本文利用一直流源換流器模擬分散式發電系統來執行實、虛功率之追蹤控制與孤島偵測，所提之主動式孤島偵測法是於 D 軸電流注入擾動訊號，而此將在市電脫離時，導致 RLC 負載終端之頻率產生偏差。再者，為改善實、虛功率追蹤控制之暫態與穩態響應及增進孤島偵測效能，本文利用兩個機率模糊類神經網路（PFNN）智慧型控制器來取代傳統比例積分（PI）控制器。最後，PFNN

網絡結構及線上學習法，注入擾動訊號孤島偵測法之可行性和有效性將於本文詳細介紹。相關收錄論文如附件。

5 月 26 日，當日會議旁聽其他專家、學者發表議題，摘錄如下：

(1) A Conceptual Framework of Integrated Evaluation Methodology for Aquaculture Lakes：

目前研究生態水資源之管理充滿許多瑣碎問題待解決，本文提供一個可大幅幫助解決其複雜性（物理，生物，生態，社會，經濟，環境等）之研究方面。本研究提供了整合與評估用於養殖湖泊參考分層理論和空間佈置各方面的影響。以結論而言，水產養殖湖泊正飽受人類活動之極大威脅，因此，人類必須認知，水產養殖湖泊是沒有任何可行方法來保持原始生態。

(2) The Taiwan Environmental Impact Assessment Act Contributes to the Water Resources Saving：

水資源短缺是目前台灣亟需解決的關鍵問題。然而，缺乏有效對水的回收與再利用和強制規範導致目前尚無法有效控制水資源。雖然現有法規針對水回收定有相當規定，但在實施和執法方面卻面臨著挑戰。因此，為了突破此窘境，本文研究的目的在於尋找適當執法方式，並提高檢測能力，建立檢測系統實現水資源的回收與再利用。台灣環境影響評價法（EIA 法）是在 1994 年公佈，其的目的是預防和減輕開發活動對環境的不利影響，以保護環境。在環評過程中，可以規範企業在不同情況下達成一定比例之水資源回收，並推展污水源減排和節水效益標準。此外，政府有權檢查企業如何處理其廢水，並根據環境評估承諾執行水資源回收，審查和測量水資源回收與再利用，以達到執行效率的目的。本文邀請權威專家在相關領域提供有關水循環再利用講座，並加強執法人員檢查知識，擬定檢查參考手冊以作為執法依據。最後，通過專家和機構間之協議，擰定最終方案與標準。這項研究旨在促進水循環再利用，也證實了環評法的環保價值。

(3) Study of Aerosol Deposition and Shielding Effects on Fluorescent Imaging Quantitative Evaluation in Protective Equipment Validation：

防護服的洩漏是職業安全衛生領域中的一個重要議題，目前沒有任何具體測量個人防護設備洩漏的定量方法。本文主要在通過使用螢光追蹤氣溶膠測量個人防護裝備的定量洩漏。螢光追蹤氣溶膠空氣微粒可由紫外光（UV）進行檢測。在經過曝光和洩漏測試之後，該個人防護裝備中除去並用紫外光掃描以評估是否有洩漏之處。因此，本文旨在建立基於螢光照明深度/氣溶膠濃度比，照明比，氣溶膠沉積和屏蔽效果，並在洩漏面積比率為防護裝備定量洩漏率的依據。

(4) Packaging Processes for the Implantable Medical Microelectronics：

用於神經疾病的電刺激醫療設備需要電性與生物相容性材料來從電極傳遞信號。而其生物周圍組織之保護特性對於長期之植入物是一個很大的挑戰。在本研究中，作者設計了最先進且具包容性、可靠性及高效率之後期過程。作者探討具有沾黏性之高質量和均勻性作為用於長期植入的生物相容性材料，這種方法能夠通過執行生物相容性材料的

保護層，以提供優好的生物相容性。

(5) Concrete Cracking Simulation Using Vector Form Intrinsic Finite Element Method：

本研究提出利用新的向量內在有限元素法（VFIFE）模擬第 1 模式下之裂紋擴展。一種結合 VFIFE 和 J 積分的領域被提出來作為計算壓力密度係數及裂紋彈性的分析，在 VFIFIE，其結構之變形是利用粒子數取代元素作表示。

5 月 27 日，當日其他學者、專家發表議題，摘錄如下：

(1) Effect of Internal Control on Fraud Detection in Public Universities in West Java Indonesia：

本文主要在研究印尼公立大學內部控制欺詐檢測和預防作為。作者採用抽樣的方法選擇大學內教職與行政同仁，同時採用簡單隨機抽樣的方法選擇大學內主官管做資料收集與回應，該問卷係專為大學工作人員設計並採封閉式問卷，並通過特殊篩選方法挑選。本文並使用統計法來描述和推斷收集的數據與分析。研究結果顯示，在印尼公立大學內部控制制度具充分性，且在統計上顯著積極的關係。

(2) Modeling and Simulation of Flow Shop Scheduling Problem through Petri Net Tools：

流程式生產排程問題（FSSP）是彈性製造系統（FMS）中生產計劃管理會面臨到的典型問題。這個問題在於找出期最佳的排程調度可以進行一系列工作，並作為一組機器或共享資源的管理。此外，所有的作業都在相同的機器排程中處理，正如所有的調度問題，其完工時間可透過操作順序或其他替代方案利用甘特圖來獲得。本文 FMS 利用派翠網路，用於建模和分析離散事件系統進行建模。最後，排程中完工時間可以透過派翠網路之令牌和矩陣獲得。

(3) Intelligent controlled doubly-fed induction generator system using PFNN：

本文以機率型模糊類神經網路(PFNN)智慧型控制器實現獨立型雙饋式感應發電系統之控制。此系統可應用於獨立供電系統，或當市電故障時作為緊急發電系統之用途。此系統在次同步、同步、超同步的情況皆能產生穩定三相電壓及頻率。本論文利用轉子側轉換器磁場導向控制，可使雙饋式感應發電機在轉速變動下皆能夠產生固定的電壓大小和頻率；利用定子側轉換器磁場導向控制，以維持直流鏈電壓的穩定。本文中詳細推導機率型模糊類神經網路智慧型控制器之網路架構及線上學習法則，並應用於雙饋式感應發電系統之轉子側及定子側轉換器，使其達到更好的暫態響應與控制效能，最後透過實驗結果來驗證所提控制方法之有效性。

參、心得報告：

本次赴日本參加國際研討會，除了可擴張自己在學術上之研究潛能，在國際觀上，對不同國家之風俗及科技發展也有新的見解與體認。在學術方面，看到許多專家學者對於現實所發生之問題提出解決方案，例如:有學者提出如何檢測個人防護裝備之洩漏問題此外，還有學者提出彈性製造系統結合派翠神經網路來找出最佳工廠之生產排程等。因此，體會到學者做研究應以解決當前所遇到之問題，以改善或增進人們生活品質。另外，在國際觀上，因本次研討會在東京舉行，其交通相當便利，因此在研討會期間利用搭乘該地區的各式鐵路系統前往會場，沿途景觀可以充分感受到日本首都的進步與繁榮，此外，對於日本人有條不紊的處理事情態度感到佩服。最後，參加國際研討會是一項很有意義的學術活動，也非常感謝科技部研的經費提供，校院部各級長官的協助，使得此次研討會能順利成行。

肆、參考資料：

圖片為研討會內外場與會議現場等

研討會地點指示牌

註冊報到

研討會場外(1)

研討會場外(2)

研討會場內(1)

研討會場內(2)

研討會場內(3)

研討會場內(4)

研討會場內(5)

研討會場內(6)

CERTIFICATE OF ATTENDANCE AND PRESENTATION

This certificate is awarded to

KUANG-HSIUNG TAN

for oral and technical presentation, recognition and appreciation of research contributions to ICEET 2016 : 18th International Conference on Electrical Engineering and Technology

Active Islanding Detection Method Using Intelligent Controller
Kuang-Hsiung Tan, Chih-Chan Hu, Chien-Wu Lan, Shih-Sung Lin, Te-Jen Chang

INTERNATIONAL SCIENTIFIC RESEARCH AND EXPERIMENTAL DEVELOPMENT

TOKYO, JAPAN

MAY 26-27, 2016

出席證明

伍、建議事項：

對於參加國際研討會，將可增進學術交流亦可開闊國際觀，利用參加國際學術研討會，使各國瞭解我們的學術成就。所謂學術無國界，藉由各國的專家學者互相研討，彼此激勵出火花，對於學術而言也是一項寶貴收穫，因此，在經費有限的情況下，期許能鼓勵老師們能多出去走走，瞭解目前各國學術研究方向，增進學校能見度，以提升自己本職學能。最後，感謝科技部研的經費提供，校院部各級長官的協助，使得此研討會能順利成行。

陸、會議資料：

收錄論文光碟片(論文電子檔 270 餘篇)

Active Islanding Detection Method Using Intelligent Controller

Kuang-Hsiung Tan, Chih-Chan Hu, Chien-Wu Lan, Shih-Sung Lin, Te-Jen Chang

***Abstract*—**An active islanding detection method using disturbance signal injection with intelligent controller is proposed in this study. First, a DC\AC power inverter is emulated in the distributed generator (DG) system to implement the tracking control of active power, reactive power outputs and the islanding detection. The proposed active islanding detection method is based on injecting a disturbance signal into the power inverter system through the *d*-axis current which leads to a frequency deviation at the terminal of the *RLC* load when the utility power is disconnected. Moreover, in order to improve the transient and steady-state responses of the active power and reactive power outputs of the power inverter, and to further improve the performance of the islanding detection method, two probabilistic fuzzy neural networks (PFNN) are adopted to replace the traditional proportional-integral (PI) controllers for the tracking control and the islanding detection. Furthermore, the network structure and the online learning algorithm of the PFNN are introduced in detail. Finally, the feasibility and effectiveness of the tracking control and the proposed active islanding detection method are verified with experimental results.

***Keywords*—**Distributed generators, probabilistic fuzzy neural network, islanding detection, non-detection zone.

I. Introduction

ISLANDING detection is an essential protection requirement for distributed generators (DGs) for personnel and equipment safety. The islanding phenomenon for the DG is defined when the DG continues to operate with local loads when the utility power is disconnected [1]. The islanding phenomenon usually occurs when the load power and the output power of the DG are balanced, i.e., the load power is entirely supplied by the DG. At this time, if the utility power is failed or interrupted, the disturbances of frequency and voltage of the DGs cannot be detected with the standard of IEEE1547or UL1741 [2], [3]. The islanding phenomenon will damage the power systems and the safety of maintenance staffs. Thus, all DG equipment is required to present an effective islanding detection method [4].

In the past decade, many literatures [5]-[8] have been proposed to prevent islanding phenomenon caused by DGs. In [5], the active frequency drift method was proposed to add dead time into the output current of the power inverter and resulted in current and voltage distortion at the point of common coupling (PCC). Thus, when the utility power is failed or interrupted, the frequency can drift beyond the non-detection zone (NDZ). In [6], the proposed active islanding detection method is based on injecting a negative-sequence current through the power inverter by means of unified three-phase signal processor. The signal cross-correlation index between the injected reactive power and the frequency deviation at the PCC is proposed to detect the islanding phenomenon in [7]. A positive feedback anti-islanding scheme using *q*-axis injection method was proposed. The method injects a disturbance signal, which contains the difference of terminal voltage, into the active power axis (*q*-axis). When the utility power is failed or interrupted, it can accelerate the voltage to drift beyond the NDZ [8]. However, the proposed method is based on the active power disturbance method for islanding detection which inherently has larger NDZ compared with the reactive power disturbance method for islanding detection [9].

Recently, the study about the integration of artificial neural network and fuzzy has been proposed in many research fields. The fuzzy neural network (FNN) owns the abilities of prediction, modeling, training, and solving problems with uncertainty [10]. Moreover, FNN does not require mathematical models and has the ability to approximate nonlinear systems [11]. Furthermore, nowadays, the new intelligent controllers, probabilistic neural network (PNNs), have also been proposed in the literatures [12]-[15]. The PNN is a feed-forward neural network and is a direct neural network implementation of Bayes classification rule and Parzen nonparametric probability density function (PDF) estimation [12]. In addition, the PNN has an inherent parallel structure, a fast training process, and guaranteed optimal classification performance if a sufficiently large training set is provided [13]. Therefore, the PNN can handle the uncertainties in industry applications effectively, and it has been widely used in nonlinear mapping, pattern classification, and classification and fault detection [14], [15]. Owing to the above advantages of PNN and FNN, the PFNN, which integrates the characteristics of PNN and FNN, has been proposed in some applications, such as stochastic modeling and control problems. In [16], the PFNN is capable of solving the uncertainties in industry applications.

In this study, a grid-connected three-phase DG system using the adopted PFNN controllers is researched for the tracking control and the islanding detection. First, a DC source power inverter is emulated the DG system to implement the tracking control of active power, reactive power outputs and the

C. C. Hu is with System Manufacturing Center, National Chung-Shan Institute of Science and Technology, Sanxia District, New Taipei City 23742, Taiwan (e-mail: huchihchan@gmail.com).

K. H. Tan is with the Department of Electrical and Electronic Engineering, Chung Cheng Institute of Technology, National Defense University, Taoyuan 335, Taiwan (corresponding author; phone: +886-3-380-9991 ext.128; e-mail: s913115@gmail.com).

C. W. Lan, S. S Lin and T. J. Chang are with the Department of Electrical and Electronic Engineering, Chung Cheng Institute of Technology, National Defense University, Taoyuan 335, Taiwan (e-mail: g941339@gmail.com; shihsunglin@gmail.com; karl591218@gmail.com).

islanding detection. Then, the characteristics of the NDZ and the proposed active islanding detection method using disturbance signal injection are introduced in detail. Moreover, the PFNNs are adopted to replace the traditional PI controllers for the tracking control and the islanding detection to improve the transient and steady-state responses of the active power and reactive power outputs of the power inverter, and the performance of the islanding detection method. Furthermore, the training algorithm based on backpropagation (BP) is derived to train the connective weights, means, and standard deviations of the membership functions in the adopted PFNN online. Finally, the adopted PFNN controllers to control the active power and reactive power outputs of the power inverter and to detect the islanding phenomenon is realized in a personal computer (PC)-based control computer via MATLAB & Simulink, and the effectiveness is verified by experimentation.

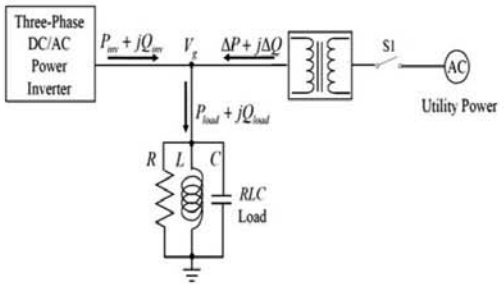

Fig. 1 Test circuit with parallel RLC load

II. Active Islanding Detection Method

A. Non-Detection Zone

The NDZ is derived from the test circuit with a parallel *RLC* resonant tank as the load as shown in Fig 1. The power flow relations of the inverter active power P_{inv}, reactive power Q_{inv}, *RLC* load active power P_{load}, reactive power Q_{load}, and utility active power ΔP, reactive power ΔQ are as follows:

$$P_{inv} = P_{load} - \Delta P;\ Q_{inv} = Q_{load} - \Delta Q. \tag{1}$$

It is difficult to detect the islanding phenomenon when active power and reactive power outputs of the grid-connected power inverter are equal to the active and reactive power of the *RLC* load, i.e., $\Delta P = 0$, $\Delta Q = 0$ [17]. When the utility power is disconnected, the added disturbance signal in the *d*-axis current will result in $Q_{inv} \neq 0$. It can be obtained as;

$$Q_{inv} = V_g^2(\frac{1}{\omega_g L} - \omega_g C) = P_{load}R(\frac{1}{\omega_g L} - \omega_g C). \tag{2}$$

where ω_g is the angular frequency of the utility power; V_g is the terminal *rms* voltage of *RLC* load. Moreover, the quality factor is defined as;

$$Q_f = R\sqrt{\frac{C}{L}} \tag{3}$$

Substitute (3) into (2), then (2) can be rewritten as follows:

$$\frac{Q_{inv}}{P_{load}} = Q_f(\frac{1}{\omega_g\sqrt{LC}} - \omega_g\sqrt{LC}). \tag{4}$$

Since the resonant frequency ω_o equals $\sqrt{1/LC}$, (4) can be rewritten as follows:

$$\frac{Q_{inv}}{P_{load}} = Q_f(\frac{\omega_o}{\omega_g} - \frac{\omega_g}{\omega_o}) = Q_f(\frac{f_o}{f_g} - \frac{f_g}{f_o}), \tag{5}$$

where f_g and f_o are the frequency of ω_g and ω_o. The NDZ is obtained with the maximum and minimum frequency defined in the IEEE Standard 1547 [2] as follows:

$$Q_f(\frac{f_{min}}{f_g} - \frac{f_g}{f_{min}}) \le \frac{Q_{inv}}{P_{load}} \le Q_f(\frac{f_{max}}{f_g} - \frac{f_g}{f_{max}}), \tag{6}$$

where $f_{\max}$ and f_{min} are the maximum and minimum frequency thresholds; $Q_f(\frac{f_{min}}{f_g} - \frac{f_g}{f_{min}})$ is the lower limit of the NDZ; $Q_f(\frac{f_{max}}{f_g} - \frac{f_g}{f_{max}})$ is the upper limit of NDZ.

B. Active Islanding Detection Method Using Disturbance Signal Injection

The proposed active islanding detection method is based on injecting a disturbance signal into the power inverter system through the *d*-axis current as shown in Fig. 2, where P_{inv}^* is the active power command of the power inverter; Q_{inv}^* is the reactive power command of the power inverter; θ is the synchronous angle obtained by phase loop lock (PLL); i_{de}^* and i_{qe}^* are the *d*-*q* axes current commands; i_{us}^*, i_{vs}^*, i_{us}^* are three-phase current commands. The errors of active power and reactive power are regulated by the PI or PFNN controllers to obtain the *d*-*q* axes current commands. Then, using the coordinate transformation algorithm, three-phase current commands can be generated. The *d*-axis current command i_{de}^* consists of *d*-axis current i_{de} and injected disturbance signal i_{dist}. The magnitude of the injected disturbance signal i_{dist} becomes stronger when the utility power is disconnected. The injected disturbance signal i_{dist} is designed as:

$$i_{dist} = k\,sign(\Delta f),\ sign(\Delta f) = \begin{cases} 1, & f[k] > f[k-1] \\ 0, & f[k] = f[k-1] \\ -1, & f[k] < f[k-1] \end{cases} \tag{7}$$

where k is the gain of disturbance signal; $sign$ is the sign function, and $sign(\Delta f)$ is determined by the frequency difference of current and last samples.

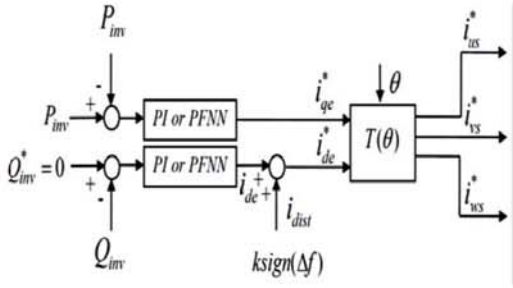

Fig. 2 Control block of proposed islanding detection method

The proposed active islanding detection method can push the frequency of the power inverter f to drift beyond the NDZ by adding the disturbance signal i_{dist} in the d-axis current i_{de} when the utility power is disconnected.

III. Probabilistic Fuzzy Neural Network Controller

Though the PI control has the advantages of simple structure and is easily implemented, the traditional PI controller is not robust in dealing with system uncertainties such as modeling errors, parameter variations and external disturbances in practical applications. Hence, in order to achieve superior effect for the proposed active islanding detection method, the online trained PFNN controllers are adopted to replace the traditional PI controllers to achieve further rapid response of the islanding detection and improve the transient and steady-state responses of the active power and reactive power outputs of the power inverter.

A. Network Structure

The adopted five-layer of the PFNN is illustrated in Fig. 3, which consists of the input layer, the membership layer, the probabilistic layer, the rule layer and the output layer. Moreover, the signal propagation and the basic function of each layer are described in detail as follows:

1. Input layer (layer 1): For every node in this layer, the node input and the node output are obtained as:

$$x_i(N) = e_i(N), \quad i = 1, 2 \tag{8}$$

where x_i represents the ith input to the input layer; N represents the Nth iteration. The inputs of the PFNN are $e_1(N) = e$ and $e_2(N) = \dot{e}$, which are the tracking error and its derivative, respectively. These nodes only pass the input signal to the next layer. In this study, the input variables are $e = P^*_{inv} - P_{inv}$ for the active power control and $e = Q^*_{inv} - Q_{inv}$ for the reactive power control.

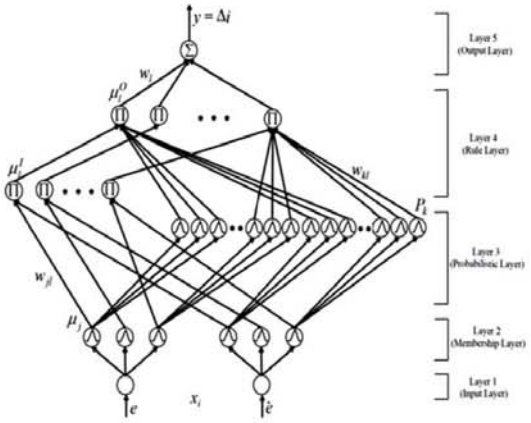

Fig. 3 Network structure of PFNN

2. Membership layer (layer 2): In this layer, the receptive field function is usually a Gaussian function in FNN. In order to reduce the computational requirements, a triangular function $f_m(x_i)$ is selected as the receptive field function. The equations of the triangular function $f_m(x_i)$ are provided as:

$$\mu_j(x_i) = f_m(x_i) = \begin{cases} 0 & \text{if } x_i \ge m_j + \sigma_j,\ x_i \le m_j - \sigma_j \\ \dfrac{x_i - m_j + \sigma_j}{\sigma_j} & \text{if } m_j - \sigma_j < x_i \le m_j \\ \dfrac{-x_i + m_j + \sigma_j}{\sigma_j} & \text{if } m_j < x_i \le m_j + \sigma_j \end{cases} \tag{9}$$
$$i = 1, 2. \qquad j = 1, 2, \ldots, 6.$$

where $\mu_j(x_i)$ is the output of the jth node of the ith input variable; σ_j is the center's width of the triangle; m_j is the center of the triangle.

3. Probabilistic layer (layer 3): For the same reason in membership layer, another triangular function $f_p(\mu_j)$ is designed as the receptive field function and its equations are provided as:

$$P_k(\mu_j) = f_p(\mu_j) = \begin{cases} 0 & \text{if } \mu_j \ge m_k + \sigma_k,\ \mu_j \le m_k - \sigma_k \\ \dfrac{\mu_j - m_k + \sigma_k}{\sigma_k} & \text{if } m_k - \sigma_k < \mu_j \le m_k \\ \dfrac{-\mu_j + m_k + \sigma_k}{\sigma_k} & \text{if } m_k < \mu_j \le m_k + \sigma_k \end{cases} \tag{10}$$
$$k = 1, 2, \ldots, 18$$

where $P_k(\mu_j)$ is the output of the kth node of the jth input variable; σ_k is the center's width of the triangle; m_k is the center of the triangle.

4. Rule layer (layer 4): In this layer, each node corresponds to a rule in the knowledge base. In the Mamdani inference, the node itself performs the product operation to obtain the inference set according to the rules as shown in (11). The probabilistic information is processed using the Bayes'

theorem [12] in consideration of the group of fuzzy grade being independent variables as shown in (12). Thus, the input and the output of this layer are described as:

$$\mu_i^I = \prod_j w_{ji}\mu_j \tag{11}$$

$$P_i^I = \prod_k w_{ki}P_k \tag{12}$$

$$\mu_i^O = \mu_i^I P_i^I \qquad i = 1, 2, \ldots, 9. \tag{13}$$

where P_i^I and μ_i^I are the input of rule layer; w_{ki} is the connective weight between the probabilistic layer and the rule layer which is set to be 1; w_{ji} is the connective weight between the membership layer and the rule layer, which is also set to be 1; μ_i^O is the output of the rule layer.

5. output layer (layer 5): In this layer, the input and the output of the node are obtained as:

$$y(N) = \Delta i = \sum_{i=1}^{9} w_i \mu_i^O \tag{14}$$

where $y(N) = \Delta i$ is the output of the PFNN; w_i is the connective weight between the rule layer and the output layer.

B. Online Learning Algorithm

According to the supervised learning algorithm, the parameter learning can be achieved by online regulate the connective weights between the output layer and rule layer, and the mean and standard deviation of the membership functions using the BP algorithm to minimize a given energy function. Hence, in order to describe the online learning algorithm of the PFNN, first the energy function E is defined as:

$$E = \frac{1}{2}(P_{inv}^* - P_{inv})^2 = \frac{1}{2}e^2 \tag{15}$$

Then, the update rules for the parameters in the PFNN are introduced as follows:

1. Layer 5: In this layer, the error term to be propagated is computed as:

$$\delta_o = -\frac{\partial E}{\partial y(N)} = -\frac{\partial E}{\partial P_{inv}}\frac{\partial P_{inv}}{\partial y(N)} \tag{16}$$

By using the chain rule, the connective weights are updated by the amount:

$$\Delta w_i = -\eta_1 \frac{\partial E}{\partial w_i} = -\eta_1 \frac{\partial E}{\partial y(N)}\frac{\partial y(N)}{\partial w_i} = \eta_1 \delta_o \mu_i^O \tag{17}$$

where the factor η_1 is the learning rate. The connective weight w_i is updated by the followings:

$$w_i(N+1) = w_i(N) + \Delta w_i \tag{18}$$

2. Layer 4: In this layer, the error terms to be propagated are described as:

$$\delta_i = -\frac{\partial E}{\partial \mu_i^O} = -\frac{\partial E}{\partial y(N)}\frac{\partial y(N)}{\partial \mu_i^O} = \delta_o w_i \tag{19}$$

3. layer 2: The error terms to be propagated are obtained by:

$$\delta_j = -\frac{\partial E}{\partial \mu_j} = -\frac{\partial E}{\partial y(N)}\frac{\partial y(N)}{\partial \mu_i^O}\frac{\partial \mu_i^O}{\partial \mu_i^I}\frac{\partial \mu_i^I}{\partial \mu_j} = \sum_i \delta_i P_i^I \tag{20}$$

By using of the chain rule, the update laws of center and center's width of the triangle are computed as follows:

$$\begin{aligned}\Delta m_j &= -\eta_2 \frac{\partial E}{\partial m_j} = -\eta_2 \frac{\partial E}{\partial y(N)}\frac{\partial y(N)}{\partial \mu_i^o}\frac{\partial \mu_i^o}{\partial \mu_i^I}\frac{\partial \mu_i^I}{\partial \mu_j}\frac{\partial \mu_j}{\partial m_j} \\ &= \begin{cases} -\eta_2 \delta_j \dfrac{1}{\sigma_j} & \text{if} \quad m_j - \sigma_j < x_i \le m_j \\ \eta_2 \delta_j \dfrac{1}{\sigma_j} & \text{if} \quad m_j < x_i \le m_j + \sigma_j \end{cases}\end{aligned} \tag{21}$$

$$\begin{aligned}\Delta \sigma_j &= -\eta_3 \frac{\partial E}{\partial \sigma_j} = -\eta_3 \frac{\partial E}{\partial y(N)}\frac{\partial y(N)}{\partial \mu_i^o}\frac{\partial \mu_i^o}{\partial \mu_i^I}\frac{\partial \mu_i^I}{\partial \mu_j}\frac{\partial \mu_j}{\partial \sigma_j} \\ &= \begin{cases} \eta_3 \delta_j \dfrac{m_j - x_i}{(\sigma_j)^2} & \text{if} \quad m_j - \sigma_j < x_i \le m_j \\ \eta_3 \delta_j \dfrac{x_i - m_j}{(\sigma_j)^2} & \text{if} \quad m_j < x_i \le m_j + \sigma_j \end{cases}\end{aligned} \tag{22}$$

where η_2 and η_3 are the learning rates. The center of the triangle m_j and center's width of the triangle σ_j are updated according to:

$$m_j(N+1) = m_j(N) + \Delta m_j \tag{23}$$

$$\sigma_j(N+1) = \sigma_j(N) + \Delta \sigma_j \tag{24}$$

The exact calculation of the sensitivity of the system $\partial E / \partial y(N)$ which is contained in $\partial P_{inv} / \partial y(N)$ and $\partial Q_{inv} / \partial y(N)$ cannot be determined due to the uncertainties of the plant dynamic such as parameter variations and external disturbances. To overcome this problem and to increase the online learning rate of the network parameters, the delta adaptation law is adopted as:

$$\delta_o \equiv e(N) + A\dot{e}(N) \tag{25}$$

where A is a positive constant.

IV. Experimentation

The block diagram of the grid-connected power inverter system for the islanding detection method is provided in Fig. 4, where C_{dc}, V_{dc}, i_{dc} are capacitor, DC link voltage and current

respectively; L_f is inductor between the power inverter and utility power; i_{ua}, i_{vg}, i_{wg} are the three-phase power inverter currents; V_{un}, V_{vn}, V_{wn} are the three-phase voltages of *RLC* load; T_a, T_b, T_c are the control signals of power inverter. The switch S1 represents the utility circuit breaker. When the S1 closes, the power inverter systems operate in grid-connected mode. On the other hand, when the S1 opens, the utility power is disconnected. The parallel *RLC* resonant load represents a local load, and the *RLC* resonant frequency is designed to 60 ± 0.1*Hz*. Moreover, when the utility frequency is 60*Hz*, the *RLC* resonant load represents a resistive load. If the utility power fails and the output power of the power inverter and the *RLC* load power are balanced, without effective islanding detection method, the output voltage and frequency of the power inverter will be maintained as same as the utility power resulting in the islanding phenomenon. Therefore, this test system can be applied to determine if the islanding detection method is valid.

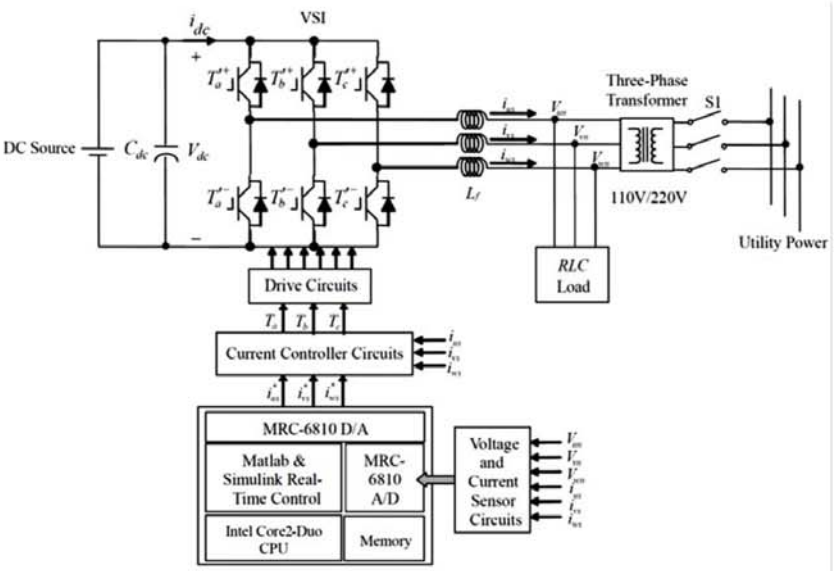

Fig. 4 Block diagram of the grid-connected power inverter system for islanding detection

In the experimentation, first, some experimental results using PI and PFNN controllers for the tracking control of the active and reactive power are demonstrated to show the control performance of the power inverter with the current injection disturbance. The experimental results of using PI controller for active power command from 0kW to 2kW and reactive power command set to be 0Var are shown in Fig. 5. In this study, the gains of the PI controller are obtained by trial and error in order to achieve good transient and steady-state control performance. The responses of active power and reactive power outputs of the power inverter are shown in Figs. 5 (a) and (b). Moreover, the experimental results using PFNN controllers for active power command from 0kW to 1kW and reactive power command set to be 0Var are shown in Fig. 6. The responses of active power and reactive power outputs of the power inverter are shown in Figs. 6 (a) and (b). From the experimental results, excellent tracking responses of both active power and reactive power can be obtained for the PFNN controller owing to the online training ability. Furthermore, the output active power and reactive power of the power inverter are not affected by the added disturbance signal. In addition, the robust control performance of the adopted PFNN controller at different operating conditions is obvious.

To verify the effectiveness of islanding detection, the utility frequency 60 Hz is designed to test the effectiveness of the proposed active islanding detection method. When the S1 shown in Fig. 4 opens, the utility power is disconnected. Fig. 7 shows the experimental results of injection disturbance method using PI controller operated at 60 Hz. The responses of frequency at the terminal of the *RLC* load and the active power output are shown in Figs. 7 (a) and (b), where P_{inv}^* is set to be 2kW and Q_{inv}^* is set to be 0Var. The utility power is disconnected at the time 1s, and the power inverter continues to deliver active power to the *RLC* load until the time 1.75s. After 1.75s, the disturbance signal is large enough to drift the frequency to shift out of the IEEE1547 scope. From Fig. 7 (a), the total time for the PI controlled power inverter stop delivering power is about 0.75s, which meets the IEEE1547 regulations (2s). Moreover, the experimental results of injection disturbance method using PFNN controller are provided in Fig. 8. The responses of frequency at the terminal of the *RLC* load and the active power output are shown in Figs. 8 (a) and (b). From the experimental results shown in Figs. 8 (a)

and (b), the total time for the PFNN controlled power inverter stop delivering power is about 0.45s, which also meets the IEEE1547 regulations. Compared with the experimental results of the proposed islanding detection method using PI controller, the responses of the proposed islanding detection method using PFNN controller are faster due to the advantages of PFNN such as online learning and quick convergence. Thus, the proposed islanding detection method using PFNN controller has excellent performance for the islanding detection.

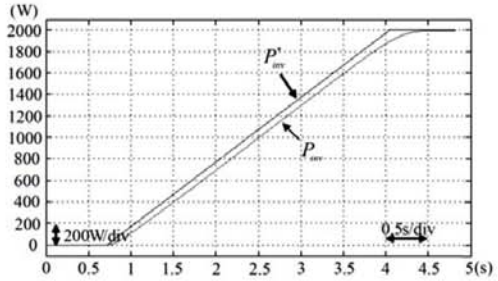

(a)

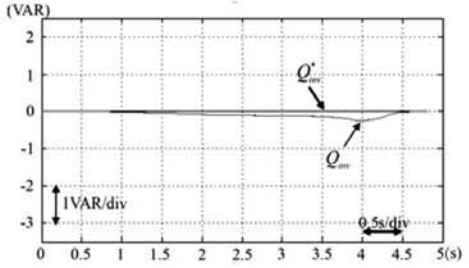

(b)

Fig. 5 Experimental results of PI controllers for tracking control, (a) responses of active power and active power command, (b) responses of reactive power and reactive power command

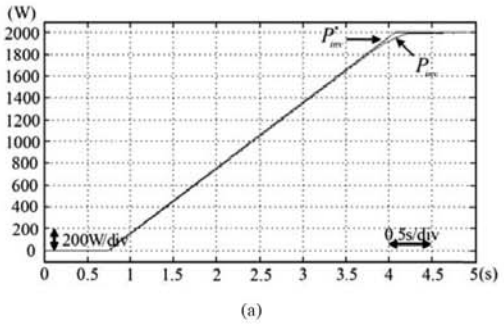

(a)

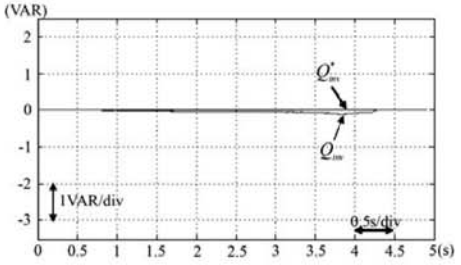

(b)

Fig. 6 Experimental results of PFNN controllers for tracking control, (a) responses of active power and active power command, (b) responses of reactive power and reactive power command

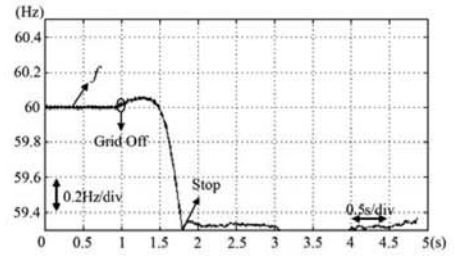

(a)

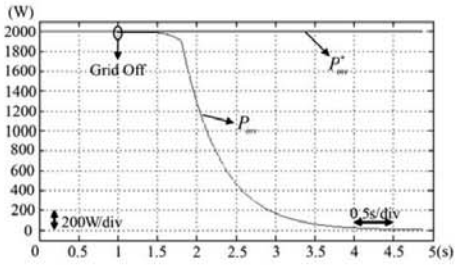

(b)

Fig. 7 Experimental results of PI controllers for proposed islanding detection, (a) frequency responses, (b) responses of active power and active power command

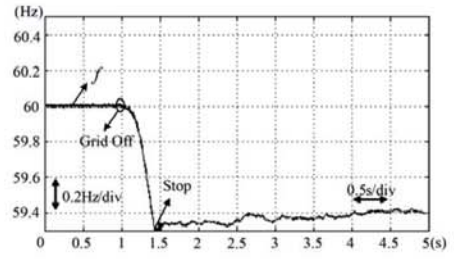

(a)

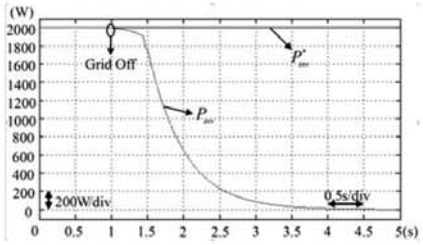

(b)

Fig. 8 Experimental results of PFNN controllers for proposed islanding detection, (a) frequency responses, (b) responses of active power and active power command

V. Conclusion

This study has successfully demonstrated the applications of the PFNN controllers on the power inverter for the tacking control of active power and reactive power outputs. Moreover, a novel islanding detection method has been successfully proposed. The proposed active islanding detection method is based on injecting a disturbance signal into the power inverter emulated the DG system through the *d*-axis current. Furthermore, the network structure and online learning algorithms of the adopted PFNN have all been described in detail. Finally, the proposed islanding detection method combined with the PFNN controller for active islanding detection has been successfully verified in the experimental results.

Acknowledgment

The author would like to acknowledge the financial support of the Ministry of Science and Technology of Taiwan through its grant MOST 103-2221-E-606-006.

References

[1] M. Ciobotaru, V. Agelidis, and R. Teodorescu, "Accurate and less-disturbing active anti-islanding method based on PLL for grid-connected PV Inverters," in *2008 Proc. IEEE Power Electronics Specialists Conf.*, pp. 4569-4576.

[2] IEEE, Std. 1547, "IEEE standard for interconnecting distributed resources with electric power systems," 2003.

[3] UL 1741, "Inverters, converters, and controllers for use in independent power systems," 2002.

[4] IEEE, Std. 929-2000, "IEEE recommended practice for utility interface of photovoltaic (PV) systems," 2000.

[5] M. E. Ropp, M. Begovic, A. Rohatgi, "Analysis and performance assessment of the active frequency drift method of islanding prevention," *IEEE Trans. Energy Conversion*, vol. 14, no.3, pp. 810–816, Sep. 1999.

[6] H. Karimi, A. Yazdani, and R. Iravani, "Negative-sequence current injection for fast islanding detection of a distributed resource unit," *IEEE Trans. Power Electronics*, vol. 23, no. 1, pp. 298–307, Jan. 2008.

[7] B. Y. Bae, J. K. Jeong, J. H. Lee, and B. M. Han, "Islanding detection method for inverter-based distributed generation systems using a signal cross-correlation scheme," *J. Power Electronics*, vol. 10, no. 6, pp. 762–768, 2010.

[8] T. T. Ma, "Novel voltage stability constrained positive feedback anti-islanding algorithms for the inverter-based distributed generator systems," *IET Renewable Power Generation*, vol. 4, no. 2, pp. 176-185, March, 2010.

[9] F. Wang, and Z. Mi, "Passive islanding detection method for grid connected PV system," in *2009 Proc. Int. Conf. on Industrial and Information Systems*, pp. 409-412

[10] Y. Gao, and M. J. Er, "An intelligent adaptive control scheme for postsurgical blood pressure regulation," *IEEE Trans. Neural Networks*, vol. 16, no. 2, pp. 475-483, March, 2005.

[11] F. J. Lin, H. J. Shieh, P. K. Huang, and L. T. Teng, "Adaptive control with hysteresis estimation and compensation using RFNN for piezo-actuator," *IEEE Trans. Ultrasonics, Ferroelectrics, and Frequency Control*, vol. 53, no. 9, pp. 1649-1661, Sept. 2006.

[12] M. Tripathy, R. P. Maheshwari, and H. K. Verma, "Application of probabilistic neural network for differential relaying of power ransformer," *IET Generation, Transmission and Distribution*, vol. 1, no. 2, pp. 218–222, March, 2007.

[13] N. Perera, and A. D. Rajapakse, "Recognition of fault transients using a probabilistic neural-network classifier," *IEEE Trans. Power Delivery*, vol. 1, no. 26, pp. 410-419, Jan., 2011.

[14] M. Tripathy, R. P.Maheshwari, and H. K. Verma, "Power transformer differential protection based on optimal probabilistic neural network," *IEEE Trans. Power Delivery*, vol. 25, no. 1, pp. 102-112, Jan., 2010.

[15] H. X. Li, and Z. Liu, "A probabilistic neural-fuzzy learning system for stochastic modeling," *IEEE Trans. Fuzzy Systems*, vol. 16, no. 4, pp. 898-908, Aug., 2008.

[16] F. J. Lin, Y. S. Huang, K. H. Tan, Z. H. Lu, and Y. R. Chang, "Intelligent-controlled doubly fed induction generator system using PFNN," *Neural Computing and Applications*, vol. 22, no. 7-8, pp. 1695-1712, 2013.

[17] A. Yafaoui, B. Wu, and S. Kouro, "Improved active frequency drift anti-islanding detection method for grid connected photovoltaic systems," *IEEE Transactions on Power Electronics*, vol. 27, no. 5. pp. 2367-2375, May, 2012.

K. H. Tan received the B.S., M.S., and Ph.D. degrees in electrical and electronic engineering from Chung Cheng Institute of Technology (CCIT), National Defense University (NDU), Taiwan, ROC in 2002, 2007 and 2013, respectively. He has been a member of the faculty at CCIT, where he is currently an assistant professor in the Department of Electrical and Electronic Engineering. His teaching and research interests include power electronics, microgrid system and intelligent control.

C. C. Hu received the B.S. and M.S. degrees in Electrical and Electronic Engineering from Chung-Cheng Institute of Technology, Taiwan in 2002, and 2007, respectively. He was received the Ph.D. degree in Electrical Engineering from National Central University, Taiwan in 2015. He has been a deputy engineer of the System Manufacturing Center at National Chung-Shan Institute of Science and Technology, and his research interests include nanophotonics, electromagnetic field simulation, near-field optics and plasmonics.

C. W. Lan was born in Tainan, Taiwan, 1981. He received the B.S., M.S. and Ph.D. degrees from the Department of Electrical and Electronic Engineering, and the School of Defense Science, Chung Cheng Institute of Technology, National Defense University, Taoyuan, Taiwan, in 2003, 2006, and 2013, respectively. He is currently an Assistant Professor of the Department of Electrical and Electronic Engineering of Chung Cheng Institute of Technology, National Defense University. His current research interests include humanoid robot, computer vision, and remote control.

S. S. Lin received the B.S. degree and the M.S. degree from the Department of Electrical Engineering, Chung Cheng Institute of Technology (CCIT) in 1997 and 2003 respectively, and the Ph.D. degree from CCIT, National Defense University (NDU) in 2010. Currently, he is an associate professor of the Department of Electrical and Electronic Engineering, CCIT, NDU, Taoyuan, Taiwan. His current research interests include Web-based automation, RFID applications, WSN-based control and monitoring applications, power monitoring systems and microprocessor systems.

T. J. Chang received the B.S., M.S., and Ph.D. degrees in electrical and electronic engineering from Chung Cheng Institute of Technology (CCIT), National Defense University (NDU), Taiwan, ROC in 1993, 2001 and 2008, respectively. He has been a member of the faculty at CCIT, where he is currently an assistant professor in the Department of Electrical and Electronic Engineering. His teaching and research interests include operating system, information security, data structure, computer network.